Available online at www.sciencedirect.com
ScienceDirect
Journal of Hazardous Materials 153 (2008) 364–371
Journal of Hazardous Materials
www.elsevier.com/locate/jhazmat

Photo-degradation of acid green dye over Co–ZSM-5 catalysts prepared by incipient wetness impregnation technique

Zeinhom M. El-Bahy [a], Mohamed M. Mohamed [b], Farouk I. Zidan [a,*], Mohamed S. Thabet [a]

[a] *Chemistry Department, Faculty of Science, Al-Azhar University, Nasr City 11884, Cairo, Egypt*
[b] *Chemistry Department, Faculty of Science, Benha University, Benha, Egypt*

Received 18 March 2007; received in revised form 21 August 2007; accepted 22 August 2007
Available online 28 August 2007

Abstract

Co–ZSM-5 catalysts with different Co-loadings (2–30 wt.%) were prepared by incipient wetness impregnation method. The prepared solid catalysts were characterized by X-ray diffraction, FTIR, *in situ* FTIR of pyridine adsorption and surface area measurements. The XRD data presented disintegration in the zeolitic crystalline structure accompanied by an increase in particle size of the prepared solids. New phases, Co_3O_4 and Co_2SiO_4, were detected with increasing the Co-loading, which indicate the strong interaction of cobalt ions with the ZSM-5 zeolite. FTIR study proved the presence of Co ions in stabilized sites inside the ZSM-5 framework. The *in situ* FTIR of adsorbed pyridine determined the type and relative strength of acidity on the surface of the prepared solids. The acidity switched from B-acid sites to L-acid sites with impregnation of cobalt ions in ZSM-5 zeolite. The acidity decreased with increasing Co-loading, which might be due to the destruction of zeolite framework and presence of new phases such as cobalt silicate and cobalt oxide on the surface. The surface texture characteristics changed with the promotion of ZSM-5 by cobalt ions, since a decrease of surface area, mean pore radius and pore volume was observed.

The assessment of the catalytic activity was performed by the use of the photo-degradation of acid green (AG) dye as a probe reaction in presence of H_2O_2 as an oxidant. The pH value controlled the degradation rate since a gradual increase of AG degradation rate was observed with increasing pH value and the optimum H_2O_2 concentration was 61.6 mmol/l. It was found that, the AG degradation rate increased until an optimum value of Co-loading (*ca.* 10 wt.%), beyond which a monotonic decrease of reaction rate was recognized. The experimental data pointed to the importance of both the cobalt moieties and the zeolite framework structure in the AG degradation reaction.

Keywords: ZSM-5; Acid green dye; Cobalt oxide; Pyridine adsorption

1. Introduction

Zeolites modified with transition metal ions have received increasing attention as promising catalysts for a variety of important reactions [1]. Zeolites can serve as hosts to activate transition metal ions, offering a unique ligand system with multiple types of coordination for cations. In addition, the restricted pore size of zeolites could limit the growth or sintering of the nanoparticles of the cation even at high temperatures [2]. Generally the zeolite structure, the type, the location of the cation and the coordination are among factors that control catalytic activity. Among the transition metal ions cobalt showed high activity towards many reactions [3–6]. It was found that the presence of other cations such as Na^+ and NH_4^+ on the Co^{2+} sitting caused deformation, and an expected reconstruction of the Si–O–A1 bridges could occur. Consequently, the acidity of the samples and specifically the Lewis acid sites will be affected. It was reported in literature that increasing the Co-loading changed the activity and durability of the Co-promoted zeolites [7–9].

Wastewaters from the textile industry are characterized mainly by intense color resulting from considerable amounts of dyes such as acid green (AG). Effective removal of color from wastewater is a serious problem since even a small amount of dye is clearly apparent. The conventional methods used for color removal are ultra filtration, extraction, adsorption and oxidation with ozone and hydrogen peroxide. Heterogeneous photocatalysis is one of the most important efficient technologies used for removal of organic contaminants from wastewater. Photocatal-

* Corresponding author.
E-mail address: zeinelbahy2020@yahoo.com (Z.M. El-Bahy).

0304-3894/$ – see front matter © 2007 Elsevier B.V. All rights reserved.
doi:10.1016/j.jhazmat.2007.08.060

ysis belongs to so-called advanced oxidation processes (AOP) [10]. AOP involves generation of a very reactive hydroxyl radical that aggressively attacks virtually all organic compounds. Photocatalytic processes are preferred due to several reasons such as: (i) complete mineralization; (ii) no waste disposal problems; (iii) no expensive oxidants needed; (iv) low costs; (v) only mild temperature and pressure are necessary [11]. Many dyes may be effectively decolorized using chemical oxidizing agents such as chlorine in the form of liquid or gas, ozone and H_2O_2 that is the most environmentally friendly oxidant [12].

The driving force of this work is to study the structural, acidic and photocatalytic properties of different loaded Co–ZSM-5 systems prepared by incipient wetness impregnation technique. Furthermore, the removal of an organic pollutant (namely acid green dye) will be tested to evaluate the relative photocatalytic activity of the prepared samples.

2. Experimental

2.1. Catalyst preparation

The impregnated Co–ZSM-5 samples were prepared by mixing calculated amount of ZSM-5 (CBr 8014, Lot no. 8014-08-D; Si/Al = 80) with an aqueous solution of cobalt nitrate ($Co(NO_3)_2{\cdot}6H_2O$, ADWIC) to give 2, 5, 10, 20 and 30 wt.% of Co/ZSM-5. The volume of solution used was that necessary to completely wet the zeolite samples. The solution temperature was adapted at 80 °C for 3 h. After impregnation the water was allowed to evaporate. It followed drying at 110 °C. The obtained solid was then calcined at 550 °C in air for 6 h. The Co-promoted ZSM-5 prepared by impregnation will be referred to as *x*Co–Z, where *x* denotes to the Co-ratio and Z refers to ZSM-5.

2.2. Catalyst characterization

The X-ray diffraction (XRD) patterns of various prepared samples were performed using a Philips diffractometer (PW 3710) with Ni-filtered copper radiation ($k = 1.5404$Å) at 30 kV and scanning speed of $2\theta = 2.5$ °/min. The crystal size of the prepared materials was determined using the Scherrer equation [13]. The crystallinity of the prepared samples was calculated using the ratio of the sum of the areas of the most intense peaks for ZSM-5 samples ($2\theta = 23°$, 23.8° and 24.3°) to that the same peaks for the standard (ZSM-5 Mobil Chemicals) and multiplying by 100. The particle size of various zeolite samples was measured using a particle size analyzer (LB-500 HORIBA, Dynamic Light Scattering).

IR spectra were recorded in the solid state as KBr pellet on Bruker (Vector 22), single beam spectrometer at room temperature. For *in situ* FTIR spectra of pyridine adsorption, a self-supporting wafer of about 30 mg/cm^2 was placed in an *in situ* FTIR quartz cell equipped with $CaCl_2$ windows and a built-in furnace. As a typical experiment the sample was thermally treated at 300 °C for 1 h under a reduced pressure of 10^{-5} Torr prior to admitting 5 Torr of pyridine at room temperature. The samples were evacuated at room temperature (RT), 100 and 150 °C and cooled before recording the spectra at RT. In each sample, the pyridine free spectrum was subtracted from the recorded spectra to evaluate the spectral changes due to pyridine adsorption.

The nitrogen adsorption isotherms were measured at −196 °C using a conventional volumetric apparatus. The specific surface area was obtained using the BET method. The surface texture characteristics were obtained from both the BET isotherm and the V_{l-t} plots.

2.3. The catalytic activity

The evaluation of the photoactivity was carried out in a cylindrical Pyrex glass reactor. A magnetic stirrer was used continuously to guarantee the good mixing of the solution. Irradiation experiments were performed using a 6 W medium pressure Hg lamp (254 nm). Unless otherwise stated, the reaction was carried out at room temperature under the conditions of 0.15 g/l of the solid catalyst in 100 ml solution of 50 ppm AG dye, 61.6 mmol/l of H_2O_2 and the pH of the solution was initially adjusted at 8. Generally, (0.1 M) HCl and (0.1 M) NaOH were used to adjust the pH value in the beginning of all experiments including the effect of pH study. The degradation of AG dye was analyzed by UV–vis spectrophotometer (JASCO V-570 unit, serial no. 29635) in the range of 190–800 nm. The degradation was determined at the wavelength of maximum absorption (622 nm). Calibration plots based on Beer-Lambert's law were established relating the absorbance to the dye concentration to determine the dye concentration during the reaction (C). In agreement with previous literature [14,15], the degradation of AG dye fitted with pseudo-first order kinetics [$\ln(C/C^0) = -kt$] (where C° and C are the initial dye concentration and its concentration at time t, respectively, and (k, min^{-1}), is the reaction rate constant). The rate constant, k, was calculated from the slopes of the straight-line portion of the plots [$\ln(C/C^0)$ vs. time].

3. Results and discussions

3.1. XRD and particles size analysis

The X-ray diffraction (XRD) patterns of Co–Z samples are shown in Fig. 1. The parent ZSM-5 showed a pattern similar to the crystalline structure reported in the X-ray data file [PDF # 79-2401]. The diffraction patterns of Co–Z samples proved that the structure of ZSM-5 was noticed in 2, 5 and 10 wt.% of Co-loading, except for a decrease of the peaks intensity. Beyond 10 wt.% of Co-loading, a great loss of zeolite crystallinity was noticed and no diffraction lines assigned to ZSM-5 structure were detected. The patterns demonstrated the disintegration of ZSM-5 structure with increasing Co-loading which was accompanied by the appearance of new lines at $2\theta = 21.0°, 31.8°, 36.0°$, 38.6° and 47.8° which are assigned to Co_3O_4 [PDF # 09-0418] and other lines at $2\theta = 29.3$, 42.4° and 56.7° which are characteristic of cobalt silicate (Co_2SiO_4) [PDF # 15-0865]. The data in Table 1 presented a marked decrease of crystallinity to ≈68, 24 and 12% for 2, 5 and 10Co–Z samples, respectively, with respect to parent ZSM-5. The addition of various amounts of

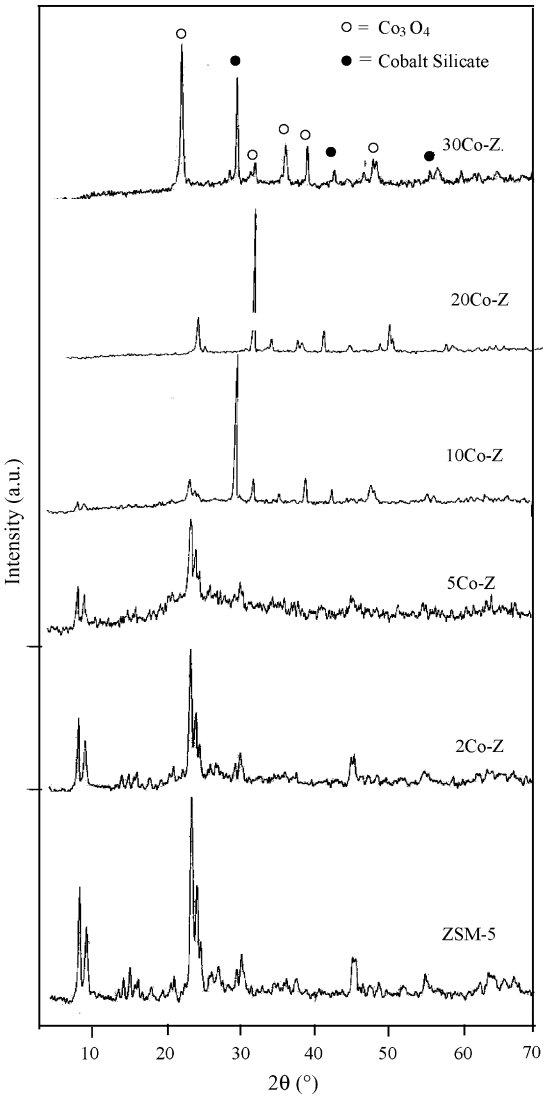

Fig. 1. X-ray diffraction patterns of parent ZSM-5 and Co–Z samples with different Co-loadings.

Co-ions caused an increase in the cell volume (Å^3) except for the 5Co–Z sample. This reflects the presence of the fraction of cobalt ions inside the zeolite pores since the ionic radius of Co ions (0.65 Å) is larger than that of Al (0.54 Å) and Si (0.26 Å) ions. It is obvious that the solids prepared by impregnation have larger particle size (D, Å) than that of parent ZSM-5, Table 1. That may be due to coagulation of cobalt moieties on the surface of the prepared catalyst.

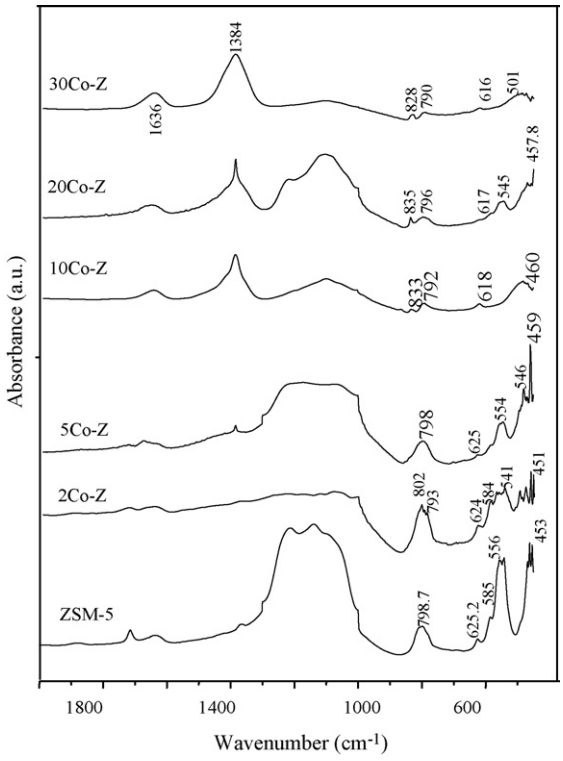

Fig. 2. FTIR spectra of parent ZSM-5 and Co–Z samples with different Co-loadings.

3.2. FTIR spectroscopy

FTIR lattice vibration spectra were used to investigate the influence of cobalt on the zeolite framework in ZSM-5 samples prepared by impregnation. Representative spectra in the range of 450–2000 cm^{-1} are shown in Fig. 2. The main peaks at 453, 556, 798 and the broad peak in the range of 1150–1250 cm^{-1} have the general assignment given by Flanigen et al. [16] for the vibrational modes of zeolite framework to the bending of the TO_4 (T = Al or Si) tetrahedra, to the structurally sensitive double five membered ring (D5R) vibration. Bonding of divalent cations to the framework oxygen atoms causes local deformation of the zeolite framework, which may be detected in T–O–T vibration changes [17,18]. The addition of 2 wt.% of cobalt caused local deformation of the vibrational band at 556 cm^{-1} while it splitted (before it fades beyond 5Co–Z) into 541 and 584 cm^{-1}. The symmetric stretching band of T–O–T vibrations at 798 cm^{-1} in ZSM-5 was shifted into 802 cm^{-1} in 2Co–Z. The deformation of the band at 556 and 798 cm^{-1} reflects the preferential

Table 1
The particle size, unit cell constants and the crystallinity calculated from XRD data of parent ZSM-5 and Co–Z samples

Sample	D (Å)	Unit cell (Å)			Cell volume (Å)^3	Crystallinity (%)
		a	b	c		
ZSM-5	286.39	19.92	20.07	13.22	5290.49	100
2Co–Z	358.5	19.94	20.35	13.38	5434.17	68
5Co–Z	318.69	19.79	20.25	13.17	5283.02	24
10Co–Z	298.76	19.72	20.29	13.29	5318.47	12

sitting of Co ions as coordinated bonding to the framework oxygen atoms. Similar result was obtained on investigating Co^{2+} ions in cationic sites of ferrierite [19]. Moreover, the absorption band at 1365 cm^{-1} confirmed the location of cobalt as coordinated framework Co^{2+} ions [20]. This band was intensified and shifted to higher wavenumber (*ca.* 1384 cm^{-1}) as the wt.% of Co^{2+} increased from 5 to 30 wt.% suggesting that H^+ or $[CoOH]^+$ might be exposed on the catalyst surface [21]. With increasing Co-loading, the intensity of the bands at 556 and 793 cm^{-1} decreased accompanied by the appearance of a new band at 833 cm^{-1} assigned to Co_3O_4. These results are in good accordance with the data obtained from XRD study since the Co_3O_4 phase was detected in the samples by increasing the Co-loading above 5 wt.%. The band at 625 cm^{-1} of (T–O) varied with Co-loadings since it had a shift to 616 cm^{-1} by increasing Co-loading up to 30 wt.% with a marked decrease in its intensity. Such changes confirmed the dealumination in the zeolite structure [22] and hence a collapse of the structure occurred. Like XRD data, the FTIR spectra point to the disappearance of the pentasil structure of ZSM-5 after 10Co–Z.

3.3. *In situ* FTIR spectra of pyridine adsorption

Acidic properties of Co-promoted ZSM-5 samples were examined using *in situ* FTIR spectroscopy of pyridine adsorption as a probe molecule. It is well known that pyridine adsorbed on Lewis acid sites (L-acid) gives bands at 1447–1460, 1488–1503, ≈1580 and 1600–1630 cm^{-1}, that on Brönsted acid sites (B-acid) at 1485–1500, 1540 and ≈1640 cm^{-1} and the hydrogen-bonded pyridine at 1400–1447, 1485–1490 and 1580–1600 cm^{-1}, respectively [23–26]. Fig. 3 shows changes occurring in the 1700–1400 cm^{-1} region of the infrared spectra of parent zeolite and Co–Z after exposure to pyridine vapor (5 Torr) at room temperature and evacuation at increasing temperatures. The *in situ* FTIR spectra of pyridine adsorbed on parent ZSM-5, Fig. 3a, were recorded after evacuation at RT, 150 and 200 °C. The spectrum recorded at RT illustrated three peaks at 1440, 1583 and 1598 cm^{-1}, which are characteristic to L-acid sites. B-acid sites were detected at 1542 and 1638 cm^{-1}. L- and B-acid sites were coming together at 1490 cm^{-1}. With increasing evacuation temperature, dramatic changes in the spectra were observed, such as the increase in the intensity of B-acid sites at the expense of Lewis ones, Fig. 3a, were observed. The increase of intensity of the bands at 1546 and 1637 cm^{-1} assigned to B-acid sites with increasing evacuation temperature may be due to the presence of isolated tetrahedral (Al(III)-OH)$^{2+}$ species. This can be interpreted in terms of hydroxyl groups extended into the large cavities, which would allow more effective coordination to pyridine ligand [27].

In the 2Co–Z sample, Fig. 3b, the spectra illustrated only L-acid sites at 1445, 1488, 1581(sh), 1598 and 1626 cm^{-1} after evacuation at room temperature. Unlike parent ZSM-5, increasing the evacuation temperature to 100, 150 and 200 °C did not lead to noticeable changes in the spectra collected except that, the peak intensities decreased slightly. This indicates a higher strength of L-acid sites on the expense of B-acid ones. From the foregoing data, one can say that the acidity was mainly B-acid sites on the parent ZSM-5 whereas it was mainly L-acid sites on the surface of Co-promoted ZSM-5. To be precise, the promotion with cobalt changes the type and strength of acidity of the prepared solids. On 5Co–Z, Fig. 3c, only a prominent band at 1598 cm^{-1} characteristic of Lewis acidity was produced. In addition, undefined small bands in the region of 1450–1500 cm^{-1} appeared and increased with increasing temperature to 200 °C to give bands at 1443, 1454 and 1484 cm^{-1}. These results indicate that Co–Z samples presented only acidity of the L-type acid sites. With exposing samples containing Co-loading higher than 5 wt.% to Py, no peaks were

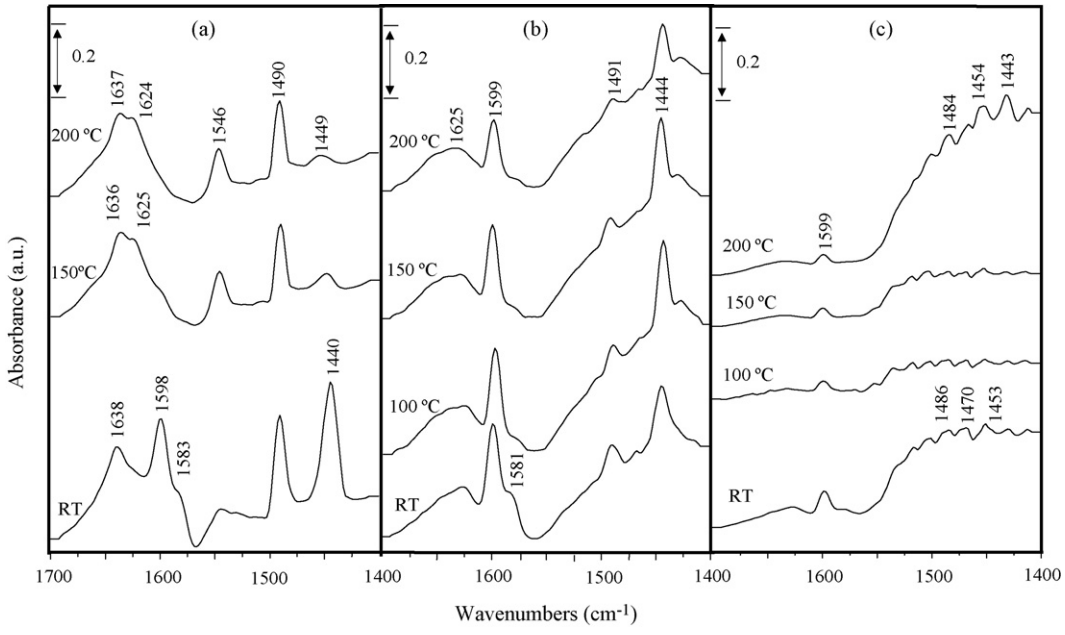

Fig. 3. *In situ* FTIR spectra of pyridine adsorption on: (a) parent ZSM-5, (b) 2Co–Z and (c) 5Co–Z evacuated at different temperatures.

Table 2
Some surface characteristics and lattice parameters of the different samples

	S_{BET} (m^2/g)	S_t (m^2/g)	$S_{(mic)}$ (cm^2/g)	$S_{(meso)}$ (cm^2/g)	$S_{(ext)}$ (cm^2/g)	V_p (cm^3/g)	$V_{(mic)}$ (cm^3/g)	$V_{(mes)}$ (cm^3/g)	r (Å)	C constant	Microporosity (%)
ZSM-5	715	704	640.5	74.46	59.7	0.618	0.553	0.064	21.61	130	89.58
2Co–Z	573	619	494	78.91	65.54	0.526	0.453	0.072	22.9	73	86.22
5Co–Z	488	346	428	59.26	38.78	0.342	0.301	0.041	17.5	5	87.85
10Co–Z	412	393	354	57.65	43.22	0.321	0.276	0.044	19.5	3	86.0
20Co–Z	434	342	361	72.39	53.3	0.283	0.236	0.047	16.3	5	83.31

noticed either at room temperature or after increasing evacuation temperature.

The decrease of the acidity of Co-promoted ZSM-5 samples with increasing Co-loading can be explained by hypothesizing that, at high concentration, Co^{2+} ions might be present as bulk oxides as well as on the surface, thus reducing coordinative unsaturated metal sites (Lewis acid sites) and the absence of proton-donor OH groups which are capable of generating Brönsted acidity. Such hypothesis was confirmed by the presence of Co_3O_4 on the surface as indicated previously by XRD and FTIR results.

3.4. Surface texture

The surface texture properties of Co–Z samples have been determined by N_2 adsorption at −196 °C and listed in Table 2. The N_2 adsorption–desorption isotherms (not shown) for all samples were found to belong to type II isotherm according to BET classification [28]. The analysis of the data of surface area and porosity of ZSM-5 before and after addition of Co ions showed that:

(i) The surface area of the prepared samples decreased monotonically with the increasing of cobalt ratio. The decrease in S_{BET} values may be due to blocking of some zeolite pores with cobalt moieties formed on the surface.
(ii) The values of S_{BET} and S_t that derived from the t-plot method are comparable to each other for the various investigated solids. This justifies the correct choice of standard t-curves used in pore analysis. Such insignificant differences showed the absence of ultramicropores in these solids at the expense of some degree of microporous characteristics.
(iii) The data of $S_{(mic)}$ and $S_{(meso)}$ (m^2/g) in Table 2 showed that the surface has mainly microporous structure with r = 6–9 Å, exceeding that noticed for neat ZSM-5 (5.5–7.5 Å).
(iv) The total pore volume decreased from 0.618 to 0.283 cm^3/g with increasing the cobalt loading to 20 wt.%.
(v) The calculated values of mean pore radius decreased with increasing the Co-loading indicating the enforcement of Co ions in the pores of ZSM-5.

In general, the surface texture data is in coherence with the XRD data of particle size. The increase of cobalt loading leads to an increase in the solid particle size and it was accompanied by a decrease in surface area, pore volume and mean pore radius. These surface texture changes are due to the presence of new phases such as Co_3O_4 and cobalt silicates, which were detected by XRD and FTIR techniques.

4. Catalytic activity of Co-promoted ZSM-5 samples

4.1. Effect of cobalt loading

The influence of cobalt loading on ZSM-5 prepared by impregnation on AG dye degradation was studied using the same above-mentioned experimental conditions, except that 0.3 g/l solid catalyst was used. Fig. 4 shows the first order plots [$\ln(C/C^0)$ vs. time] of the AG degradation over Co–Z with different Co-loadings (*ca.* 0–30%). The rate constant values, k (min^{-1}), calculated from the straight-line portion of the first order plots as a function of the Co wt.% are listed in Table 3. From these data, a general enhancement of the degradation efficiency of AG dye with increasing the cobalt loading in the range 2–10 wt.% was noticed. The dye degradation was approximately 93% after 5 min of the reaction over 10Co–Z catalyst. Increasing Co-content beyond 10% leads to a decrease of the catalytic activity. It is noteworthy to mention that the catalytic activity of 10Co–Z (0.16 min^{-1}) was approximately ≈40 times higher compared to the parent ZSM-5 (0.004 min^{-1}).

The amount of leached Co^{2+} measured by atomic absorption (Varian, AA 220) was found to be 2.6 ppm. To determine whether

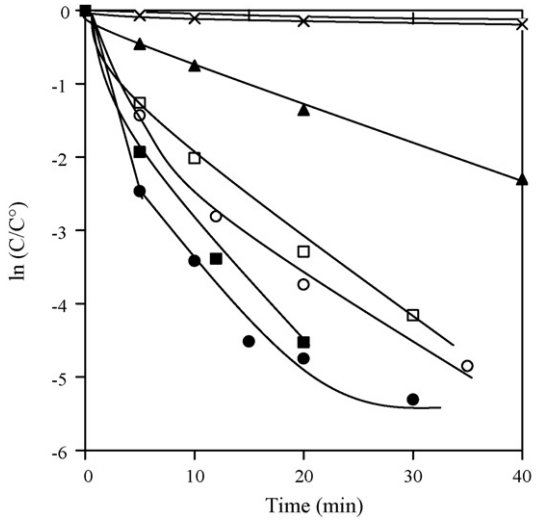

Fig. 4. First-order plots of AG degradation over Co–Z catalyst with different Co-loadings: 0% (×), 2% (▲), 5% (□), 10% (●), 20% (■), 30% (◯) and 3 ppm Co^{2+} (+); using: 0.3 g catalyst, 50 ppm dye concentration, pH 8, 61.6 mmol/l H_2O_2.

Table 3
Reaction rate constant of AG degradation as a function of Co-loadings

Co (wt.%)	k (min^{-1})
0	0.004
2	0.05
5	0.115
10	0.16
20	0.14
30	0.10

the homogeneous degradation of AG by Co^{2+} takes place or not, the catalytic activity of 3 ppm Co^{2+} was measured under the same above-mentioned experimental conditions. No remarkable activity was noticed due to the presence of Co^{2+} ions as shown in Fig. 4. It can be concluded that the AG degradation does not occur homogeneously in presence of Co^{2+} and the rate of reaction is mainly due to heterogeneous and not homogeneous catalysis.

The order of catalytic activity is different from that of the Co-ratio. This result nullifies the sole dependence of the catalytic activity on cobalt species in the solid catalyst. As mentioned before, the catalytic activity was maximum over the 10Co–Z catalyst. The XRD data showed that a residual crystallinity of Co–Z catalysts remained up to 10 wt.% of Co-loading, after which a collapse of the zeolite structure was observed. The role of the zeolite might be correlated with the adsorption process, in the sense of high surface area and the decrease of particle size. However, a noticeable increase in the photocatalytic activity of 10Co–Z may also be due to other phases such as Co_3O_4 and Co_2SiO_4 beside zeolite structure, since Co_3O_4 has high oxygen mobility, which correlates well with the oxidation capability. From the foregoing discussion, it is clear that catalytic activity mainly depends on both the cobalt species (Co_3O_4 and Co_2SiO_4) and the zeolite framework structure, the combination of which is optimal for the sample containing 10 wt.% of cobalt.

It was necessary to prepare cobalt silicate and Co_3O_4 species to check their photocatalytic efficiency, either individually or as a mixture of both at a molar ratio of 1:1. The activity under the same experimental conditions was found to be very low compared with 10Co–Z. However, the Co_3O_4/cobalt silicate mixture gave a rate constant value of 0.042 min^{-1}, which is one-fourth of that obtained for 10Co–Z under the same experimental conditions. These data clearly reveal the importance of cobalt ions together with zeolite in the photocatalytic degradation of AG dye.

4.2. The influence of the amount of catalyst

As previously mentioned, the catalyst 10Co–Z exhibited the highest catalytic activity. Therefore, the effect of the amount of 10Co–Z on AG dye degradation was studied, and the first order plots of the studied reaction are shown in Fig. 5. The rate constant values (k, min^{-1}) as a function of the catalyst mass are presented in Table 4. It can be seen that the degradation rate increases gradually with increasing the mass of catalyst used in each run. Moreover, almost complete degradation of AG dye

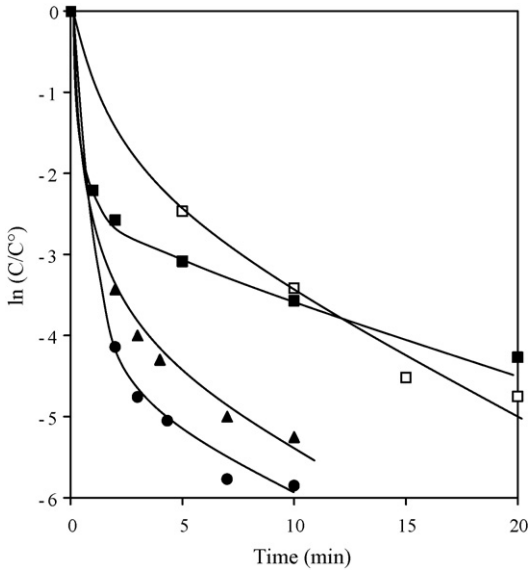

Fig. 5. First-order plots of AG degradation over different amounts of 10Co–Z catalyst using: 50 ppm dye concentration, pH 8, 61.6 mmol/l H_2O_2: (■) 0.15, (□) 0.3, (▲) 0.5 and (●) 1 g of 10Co–Z catalyst.

was observed after 10 min in the presence of both of 0.5 and 1 g/l catalyst. Thus, one may use 0.5 g/1 as minimum concentration to attain effective color removal in few minutes. The acid green degradation was studied over TiO_2 [15] and the maximum degradation was attained for 2 g/l of TiO_2 concentration since complete decolorization of 80 μM (40 ppm) of the dye (M_w = 496 g/mol) was noticed in 15 min. In the present work, 50 ppm was completely decolorized after 10 min in the presence of 0.5 g/l of the employed catalyst, 10Co–Z. Consequently, it is apparent that, the catalytic activity of the prepared catalyst may be four times more than that of the previous employed catalysts for the same reactants.

Although the leached amount of Co^{2+} increases with increasing the amount of catalyst (*ca*. 3.2 ppm in case of 1 g/l catalyst), the catalytic activity remained almost constant. Again, the forgoing results suggest the absence of homogeneous catalysis by Co ions and support the above-mentioned finding in the previous section. It is also important to note that the activity did not change much with increasing the amount of catalyst, which may be due to the aggregation of solid particles while using large amount of catalyst. Accordingly, a decrease of the number of surface active sites and an increase of opacity and light scattering of Co–Z particles occurred. Hence, a decrease in the passage of radiation through the sample and a decrease in the degradation rate will certainly happen [29]. Therefore, use of the

Table 4
Reaction rate constant of AG degradation as a function of the amount of the catalyst

Catalyst mass (g)	k (min^{-1})
0.15	0.12
0.3	0.16
0.5	0.29
1	0.31

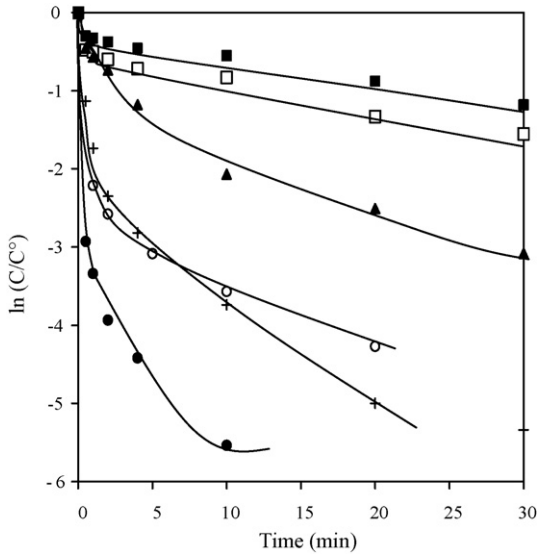

Fig. 6. First-order plots of AG degradation over 10Co–Z catalyst and using: 61.6 mmol/l H_2O_2, 0.15 g/l catalyst, 50 ppm dye concentration at different pH values: pH 2 (□), 3 (■), 7(▲), 8 (◯), 9(+), 10.4 (●).

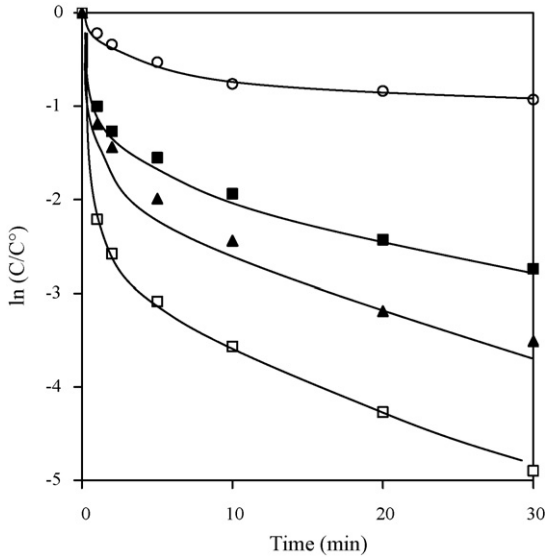

Fig. 7. First-order plots of AG degradation over 10Co–Z catalyst using: 0.15 g/l catalyst, 50 ppm dye concentration, pH 8 and different H_2O_2 concentrations: (◯) 0, (■) 29, (□) 61.6 and (▲) 108 mmol/l H_2O_2.

optimum amount of catalyst, 0.5 g/l. This will not only decrease the reaction time but also prevent another source of pollution, which comes from the leached cobalt ions.

4.3. Influence of pH on the AG dye degradation

Fig. 6 presents the first-order plots of AG degradation over 10Co–Z using different initial pH values in the range of 2–10.4 using the same experimental conditions as above-mentioned. It is clear that the degradation of the dye increases with raising pH. This is also simplified in Table 5 where the degradation rate constant (k, min^{-1}) is listed as a function of pH. It is apparent that the rate of degradation was pH dependent and the activity increased with increasing pH value. The maximum degradation (100%) was achieved over 10Co–Z after 5 min reaction time at pH 10.4. It is well known that, AG dye has a sulfuric group (negatively charged) as well as aryl methane (positive charge nitrogen) in the structure. Thus in alkaline solution, interaction between catalyst surface (Si–O^-) and dye (specifically the nitrogen group) favors the adsorption of the dye on the surface and accordingly the photocatalytic activity increases. On the other hand, an expected charge matching mechanism based on the compensation of the ionic charges (like Na^+ ones) between the catalyst surface (Si–O^-) and the SO_3 group could be obtained. At high pH, the hydroxyl radicals can be formed by the reaction between hydroxide ions and positive holes. The positive holes are considered as the predominant species at neutral or high pH. It was reported in the literature [30,31] that in alkaline solution $^{\bullet}OH$ are easier to be generated as the holes oxidize more hydroxide ions available on the employed catalyst surface. Thus, the efficiency of the process is logically enhanced since the oxidizing agent [$^{\bullet}OH$] concentration will increase [32].

Table 5
Reaction rate constant of AG degradation as a function of pH value

pH	k (min^{-1})
2	0.034
3	0.024
7	0.109
8	0.12
9	0.14
10.4	0.38

4.4. The influence of H_2O_2 concentration

Due to the importance of the presence of an oxidant such as H_2O_2 in the photocatalytic reactions, a study of the effect of the variation of H_2O_2 concentration should be carried out using the above-mentioned experimental conditions. The plot of [$\ln(C/C^0)$ vs. time] at different H_2O_2 concentrations is shown in Fig. 7 and the slopes of the straight-line part (k, min^{-1}) are presented in Table 6. The presence of H_2O_2 accelerated the AG degradation rate till an optimum concentration of 61.6 mmol/1. This can be explained by the effect of the $^{\bullet}OH$ radicals produced efficiently from H_2O_2 decomposition until being maximum at the concentration of 61.6 mmol/l of H_2O_2. On the other hand, the decrease of the degradation rate upon further increasing the H_2O_2 concentration could be due to the generation of hydroperoxyl radicals ($HO_2^{\bullet}$), which are much less reactive and do not contribute to the dye degradation that occurs only by reaction with $^{\bullet}OH$ radicals [33]. Furthermore, the increase of H_2O_2 concentration may

Table 6
Reaction rate constant of AG degradation as a function of H_2O_2 concentration

H_2O_2 (mmol/l)	k (min^{-1})
0	0.03
29	0.08
61.6	0.12
108	0.10

lead also to scavenge the •OH radicals and consequently inhibits the AG dye degradation as well.

5. Conclusions

The structural changes due to the impregnation of different cobalt ratios loaded on ZSM-5 zeolite were studied. The incorporation of cobalt ions to ZSM-5 led to strong interaction of cobalt with ZSM-5 structure. The XRD and FTIR data detected a decrease of ZSM-5 structure, followed by a collapse of MFI framework when increasing the cobalt ratio above than 10 wt.%. The catalyst characterizations verified that cobalt ions bonded to the framework oxygen atoms and caused a local deformation of the pentasile structure. The acidity of the prepared catalysts decreased with increasing the Co-content until no pyridine adsorption was noticed beyond 5 wt.% of Co-loading.

The catalytic activity increased monotonically with increasing the Co-loading and it was maximum at 10 wt.%, which has catalytic activity 40 times higher than that of parent ZSM-5. The AG degradation was correlated with the zeolite characteristics and the cobalt moieties in the catalyst. It was concluded that the presence of both cobalt moieties and MFI structure is necessary for AG degradation. In other words, the interaction between cobalt moieties and zeolite is very important to perform the studied catalytic reaction. The catalytic activity has a good correlation with the pH value due to the increase of •OH that comes from the reaction $OH^- + h^+ \rightarrow {}^\bullet OH$.

References

[1] M.C. Dalconi, A. Alberti, G. Gruciani, P. Ciambelli, E. Founda, Micropor. Mesopor. Mater. 62 (2003) 191.
[2] I. Othman, R. Mohamady, I.A. Ibraheem, M.M. Mohamed, Appl. Catal. A 299 (2006) 95.
[3] Y. Li, J.N. Armor, J. Catal. 150 (1994) 376.
[4] M.C. Campa, S.D Rossi, G. Ferraris, V. Indovina, Appl. Catal. B 8 (1996) 315.
[5] A.Y. Stakheev, C.W. Lee, S.J. Park, P.J. Chong, Appl. Catal. B 9 (1996) 65.
[6] J. Dedecek, D. Kaucky, B. Wichterlova, Micropor. Mesopor. Mater. 35–36 (2000) 483.
[7] X. Wang, H.Y. Chen, W.M.H. Sachtler, Appl. Catal. B 26 (2000) L227.
[8] Y. Chang, A. Sanjurjo, G. Krishan, B. Woods, E. Washsman, Catal. Lett. 57 (1999) 187.
[9] F. Witzel, G.A. Sill, W.K. Hall, J. Catal. 149 (1994) 229.
[10] R. Munter, S. Preis, J. Kallas, M. Trapido, Y. Veressinina, Kemia-Kemi/Finn. Chem. J. 58 (2001) 354.
[11] P.K. Malik, S.K. Sanyal, Sep. Purif. Technol. 36 (2004) 167.
[12] A.H. El-Daly, M.H. Abdel-Fattah, A.M.B. El-Din, Dyes Pigments 66 (2005) 161.
[13] P. Klug, L.E. Alexander, Direction Procedures for Polycrystalline and Amorphous Materials, Wiley, New York, 1954.
[14] A.M. Daifullah, M.M. Mohamed, J. Chem. Technol. Biotechnol. 79 (2004) 468.
[15] M.R. Ghezzar, F. Abdelmalek, M. Belhadj, N. Benderdouche, A. Addou, Appl. Catal. B 71 (2007) 304.
[16] E.M. Flanigen, H. Khatami, H.A. Szymanski, Adv. Chem. Ser. 101 (1971) 201.
[17] R. van Santen, Adv. Solid State Chem. 1 (1989) 151.
[18] V. Sundaramurthy, N. Lingappen, J. Mol. Catal. A 160 (2000) 367, and references stated therein.
[19] Z. Sobalik, J. Dedecek, I. Ikonnikov, B. Wichterlova, Micropor. Mesopor. Mater. 25 (1998) 225.
[20] A. Auroux, G. Goudurier, R. Shannon, J.C. Vedrine, in: S. Portyka, M. Lindhemer (Eds.), Proceedings of the AFCAT Meeting, vol. 16, Montpellier, 1987, p. 68.
[21] J.L. Schlenker, J.J. Pluth, J.V. Smith, Mater. Res. Bull. 14 (1979) 751.
[22] M.M. Mohamed, T.M. Salama, J. Colloids Interf. Sci. 249 (2002) 104.
[23] M.I. Zaki, M.A. Hasan, F.A. Al Sagheer, L. Pasupulety, Colloids Surf. A 190 (2001) 261.
[24] P. Pitchat, M.V. Mathieu, B. Imelik, Bull. Soc. Chem. Fr. 8 (1969) 2611.
[25] L.H. Little, Infrared Spectra of Adsorbed Species, Academic Press, London, 1966, pp. 193–198.
[26] M. Sasidharan, S.G. Hegde, R. Kumar, Micropor. Mesopor. Mater. 24 (1998) 59.
[27] T.M. Salama, I. Othman, M.S. Sirag, G.A. Shobaky, Micropor. Mesopor. Mater. 95 (2006) 312.
[28] S. Brunauer, The Adsorption of Gases and Vapors, Oxform University Press, Oxford, 1944.
[29] A.P. Toor, A. Verma, C.K. Jotshi, P.K. Bajpai, V. Singh, Dyes Pigments 68 (2006) 53.
[30] C.R. Lopez, G.E. Abel, L.I. Marta, Chemosphere 48 (2002) 393.
[31] W. Chung-Hsin, Chemosphere 57 (2004) 601.
[32] M.H. Habibi, A. Hassanzadeh, S. Mahdavi, J. Photochem. Photobiol. A 172 (2005) 89.
[33] G.V. Buxton, C.L. Greenstock, W.P. Helman, A.B. Ross, W. Tsang, J. Phys. Chem. Ref. Data 17 (2) (1988) 513.